Inelastic neutron scattering measurements on the transverse acoustic and lowest optic modes in $KTaO_3$ doped with lithium

1996 J. Phys.: Condens. Matter 8 1109

(http://iopscience.iop.org/0953-8984/8/9/004)

J. Phys.: Condens. Matter **8** (1996) 1109–1121. Printed in the UK

Inelastic neutron scattering measurements on the transverse acoustic and lowest optic modes in $KTaO_3$ doped with lithium

R S Klein†, G E Kugel† and B Hennion‡

† Laboratoire Matériaux Optiques à Propriétés Spécifiques, Centre Lorrain d'Optique et Electronique des Solides, Université de Metz et Supélec - 2, rue E. Belin, 57078 Metz Cédex 3, France

‡ Laboratoire Léon Brillouin, CEA–CNRS de Saclay 91191 Gif-sur-Yvette Cédex, France

Received 24 July 1995, in final form 16 October 1995

Abstract. Two crystals of $KTaO_3$:Li with 1% and 5% Li have been investigated by inelastic neutron scattering. The transverse acoustic and lowest optic modes have been measured in the [100] direction from room temperature down to 10 K. The wavevector dependences of the mode softening, damping and intensities are represented. The measured dispersions are analysed in the framework of an extended shell model assuming an anisotropic non-linear polarizability of the oxygen ion. On the basis of this model, structure factors are calculated and compared with measured phonon intensities. Conclusions on the influence of the lithium substitution on the non-linear character of the polarizability are discussed.

1. Introduction

The mixed $K_{1-x}Li_xTaO_3$ (KTL) system is considered as a prototype system of a dipole glass especially in the low-Li-concentration ($x < 0.04$) range [1, 2]. In this system, the Li^+ ions are substituted for the K^+ ions, but by occupying off-centre positions in the oxygen cage of cubic symmetry. The small Li^+ ions (Li ionic radius about 0.6 Å) reside on six equivalent positions, each displaced by about 1 Å in the ⟨100⟩ directions [3] from the substituted K site (ionic radius, about 1.33 Å), forming consequently dipolar electric and quadrupolar elastic moments [1, 2].

The KTL system has already been studied by several experimental methods such as x-rays [4], birefringence [5], Brillouin [6] and Raman spectroscopy [7, 8] and second-harmonic generation [9]. Dielectric [10–12] and recent acoustic measurements [13–15] have also been performed. Nevertheless, in this system, the nature of the low-temperature phase as well as the mechanisms of the transition leading to it are still controversial.

Additional inelastic neutron scattering measurements are proposed here as a complementary method of studying this system. Several workers have used this method to characterize pure $KTaO_3$ [16–19] and $KTaO_3$ doped with niobium (KTN) [20–23], but only three articles on neutron studies of the KTL system exist. In the first article, Kamitakahara *et al* [24] have essentially studied the neutron Bragg-reflection intensities for 1.7 and 4% KTL crystals as a function of temperature, time and electric field. In the second article, neutron diffraction measurements of the Bragg intensities of a sample with 3% Li were presented by Maglione *et al* [25]. Their results were interpreted in terms of strain distribution

0953-8984/96/091109+13$19.50

and characteristic size of the dipolar regions. More recently, Toulouse and Hennion [26] reported elastic neutron scattering measurements on 3.5% Li KTL in the presence of an electric field; they found a splitting of the transverse acoustic (TA) branch, below the phase transition temperature, into *a* and *c* polarized phonons and concluded that a transition from a cubic to a tetragonal ferroelectric phase occurs in 3.5% Li KTL. The TA branch splitting has been compared with earlier results obtained on the lowest transverse optic (TO_1) mode measured by Raman scattering [8]. Nevertheless, this optic mode has up to now not been investigated by neutron scattering measurements.

In this paper a complementary study is presented. The TA mode and the TO_1 mode have been measured in the [100] direction up to the Brillouin zone boundary. These measurements have been performed between room temperature and 10 K for samples with 1% Li and 5% Li, respectively. They allow the determination of the dispersion and damping of these transverse modes and their evolution with temperature and Li concentration. These results, together with other neutron scattering results obtained on pure $KTaO_3$ and on KTN and with Raman scattering data obtained on the same crystals, provide the experimental basis for the theoretical considerations. A non-linear lattice dynamical model gives fair agreement with the measured dispersion curves. In the next section we shall briefly present the experimental conditions and data analysis procedure. The analysed results will be described in section 3, the model and the comparison between experimental data and calculations will be presented in section 4, and conclusions will be drawn in section 5.

2. Experimental conditions and fitting procedure

Inelastic neutron scattering measurements have been performed on the triple-axis spectrometer lt installed on a thermal beam of the Orphee reactor at the Laboratory Léon Brillouin in Saclay (France). The monochromator and analyser were pyrolytic graphite in the [002] reflection. The monochromator was vertically bent and the analyser horizontally bent with no collimators on the neutron path. Due to the geometry of the spectrometer, this corresponded to natural collimations of about $25'/35'/50'/50'$. The measurements have been performed at a constant $k_f = 2.662$ Å^{-1} which yielded an energy resolution (FWHM) varying from 0.24 THz for elastic scattering to 0.45 THz for an energy transfer of 5 THz. A graphite filter on k_f prevented higher-order contamination.

Two $K_{1-x}Li_xTaO_3$ crystals with $x = 0.01$ and $x = 0.05$ have been investigated. The sample dimensions were 5 mm × 5 mm for $x = 0.01$ and 4 mm × 5 mm × 5 mm for $x = 0.05$. The scattering plane was of (100) type and measurements were carried out along $[2\xi 0]$ to obtain the TA mode and the TO_1 mode in a temperature range from room temperature down to 10 K.

All the data have been analysed to obtain as far as possible physically meaningful parameters. The neutron scattering cross section for phonons has been obtained in the form of a damped harmonic oscillator. The calculated lineshape obtained by folding this cross section with the resolution function of the spectrometer was fitted to the data by adjusting the frequency, damping and strength (proportional to the dynamical structure factor) of the measured point. This was a reasonable assumption except for the TA branch at low wavevector values where the focusing effect was important. The resulting decrease in the energy linewidth made clearly visible an asymmetric lineshape resulting from the curvature of the dispersion surface when going away from the [100] direction. We use for this curvature an estimate obtained in previous neutron measurements [26] and we accounted for it in the lineshape calculation.

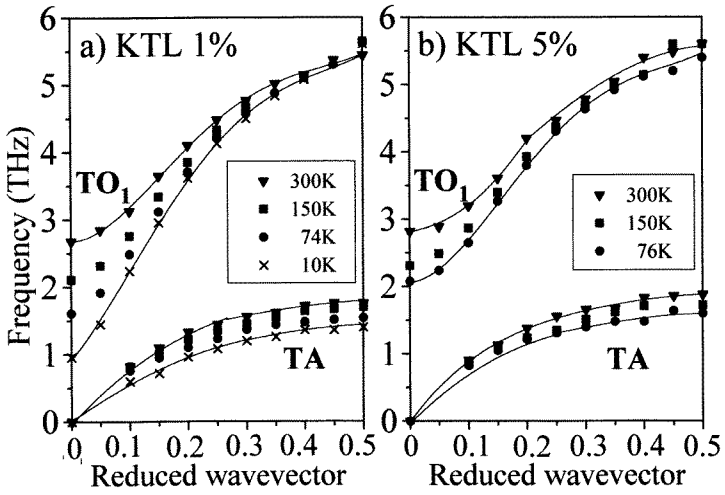

Figure 1. Dispersion curves of the TO_1 and TA modes (a) for 1% Li KTL between 300 and 10 K and (b) for 5% Li KTL between 300 and 76 K. The lines are guides to the eye.

3. Experimental results

3.1. Dependence of the dispersion curves on temperature and Li concentration

In figure 1 are reported the measured TA and TO_1 mode dispersion curves for several temperatures in both crystals. An important softening is visible, affecting the whole branch for the TA mode and the small q-value part for the TO_1 mode. This kind of softening has already been observed in pure $KTaO_3$. To appreciate the dependence on Li substitution, figure 2(a) and 2(b) display our results for the TO_1 mode at room temperature and $T = 10$ K, respectively, together with those of pure $KTaO_3$ [16–18] and $KTaO_3$ doped with 8% Nb [22, 23]. At room temperature, the phonon dispersion is only slightly affected by substitution, but the $T = 10$ K data clearly show the importance of substitution on the softening of the whole TO mode. The substitution by Nb enhances the softening while the substitution by Li decreases it. Such a reduction in the softening of the TA mode is also observed when increasing the Li concentration from 1% to 5%. Moreover this increase is accompanied by the appearance of a structural transition which leads to a splitting of the TA and TO modes in the 5% KTL. We shall come back to this point later. To complete the description of the evolution of the TO softening, we have reported in figure 3 the data at $q = 0$ known from neutron scattering studies (this study and [16–18]) and of Raman [8] or hyper-Raman [27, 28] spectroscopy.

3.2. Cubic–tetragonal transition in 5% Li KTL

In the 5% Li KTL, a splitting of the TO mode is clearly observed when the temperature is decreased. This is illustrated in figure 4 where the scattered intensities in 1% Li KTL and 5% Li KTL at room temperature and at 10 K are compared. A similar splitting of the TA mode is observed. Such a splitting has already been reported for the TA mode of 3.5% Li KTL by Toulouse and Hennion [26]. This reflects the occurrence of a transition towards a low-temperature tetragonal phase. In this phase, the a^* and c^* directions are not

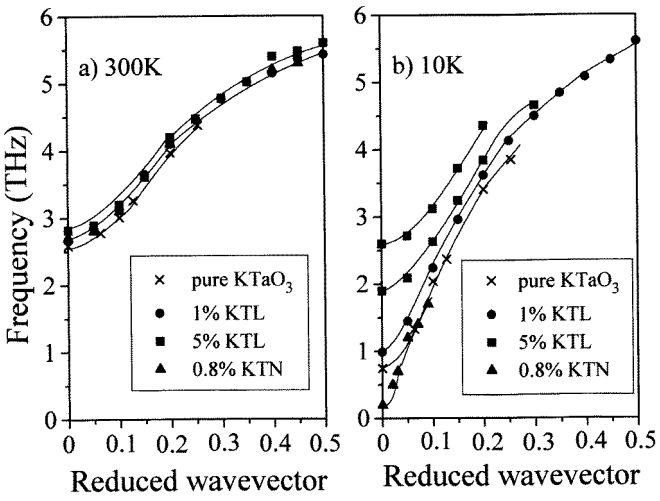

Figure 2. Comparison of the dispersion curves of the TO_1 mode in pure $KTaO_3$ [16, 18] 0.8% Li KTN [22, 23] and in 1% and 5% Li KTL for (a) 300 K and (b) 10 K. The lines are guides to the eye.

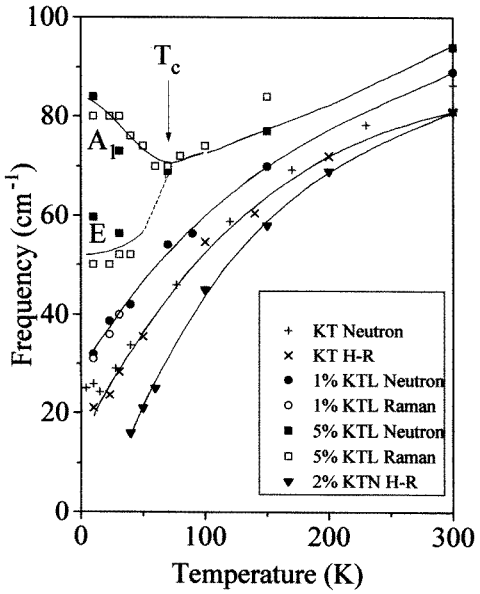

Figure 3. Comparison of the TO phonon frequencies at $q = 0$ as a function of temperature for pure $KTaO_3$ [16, 17, 27, 28], 2% Li KTN [28], 1% Li KTL and 5% Li KTL. The lines are guides to the eye.

equivalent and a superposition of two different dispersions is observed due to the coexistence of domains inside the sample. The values obtained for the TO mode are in good agreement with those obtained by Raman scattering in the same sample. The transition temperature has been determined on the same sample by ultrasonic measurements [13] and is $T_c = 75$ K.

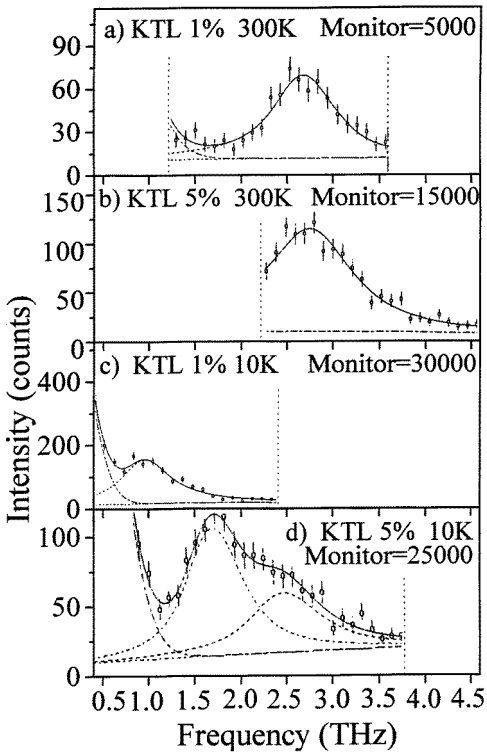

Figure 4. Experimental (ϕ) and fitted (——, – – –) neutron groups corresponding to zone-centre ($q = 0$) TO phonons at $q = 0$ (a), (c) for 1% Li KTL at (a) 300 K and (c) 10 K and (b), (d) for 5% Li KTL at (b) 300 K and (d) 10 K. In (d), the neutron groups represent two branches in different non-equivalent [100] directions which are observed in the given scattering geometry due to the multidomain structure of the sample below the cubic–tetragonal phase transition.

Below T_c, the A_1 symmetry component hardens while the E component softens as shown in figure 3. Such an observation has been made by Prater *et al* [8] in 5.4% Li KTL below 68 K. The variation in the lattice parameter has been measured by x-ray diffraction [4] and found to be quite small ($\Delta c/a = 1.4 \times 10^{-3}$) in comparison with the variation in the frequencies of the A_1 and E modes ($\Delta\omega/\omega = 0.35$).

The same phenomenon has been observed for $KNbO_3$ where a cubic–tetragonal phase transition occurs at 435 °C [29].

In figure 5 are reported the split TA and TO modes at 10 K. The results obtained at 31 K are given in the inset. Due to the limited resolution, the determination of the TA splitting is not very precise, particularly because of the asymmetric lineshape of the scattering at small q-values. The indicated values have been obtained under the assumptions of identical damping of the two modes and a 2:1 ratio due to the equipartition of the domains. These assumptions have been used and proved to be consistent with [26]. The splitting is found to be uniform ($\Delta\omega/\omega = 0.22$) between $q = 0.15$ and the zone boundary. For the TO mode, the same analysis yields a decrease in the splitting between $q = 0$ and $q = 0.2$ but could not be ascertained at larger q-values when it becomes comparable to the resolution of the measurement. Measurements at $T = 31$ K still reveal these splittings but nevertheless with reduced values, which makes it difficult to determine precisely the position of the upper

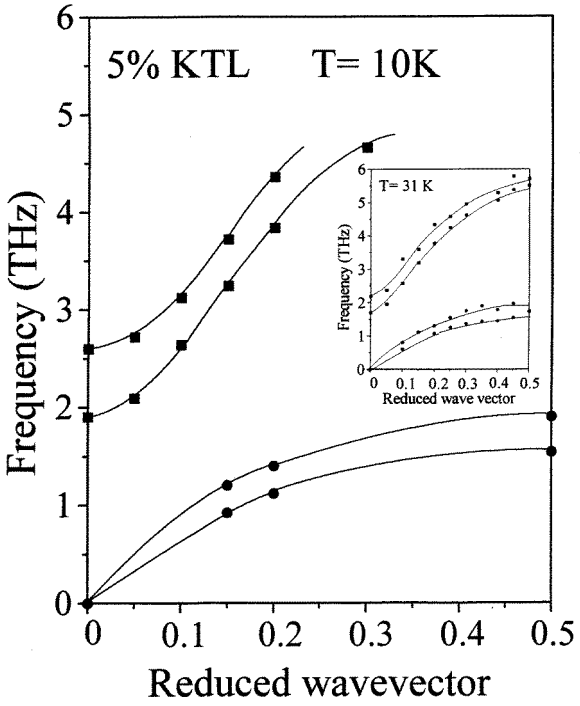

Figure 5. Dispersion curves of the TO_1 and TA modes for 5% Li KTL at 10 K. The dispersion curves obtained at 31 K for 5% Li KTL are given in the inset. The lines are guides to the eye.

modes exhibiting intensities half of the lower modes. The main proof of this splitting is the abnormal linewidth found for the modes when analysed with the assumption of unsplit branches.

3.3. Temperature and wavevector dependences of the dampings and intensities

In figures 6(a) and 6(b), the damping of the TO phonon at 300 and 10 K is represented as a function of reduced wavevectors for 1% Li KTL and 5% Li KTL, respectively. In the two samples, the damping remains constant at low wavevectors and then decreases rapidly for $0.15 < \xi < 0.3$. These values correspond to a phonon wavelength of between three and six lattice parameters.

The correlation length of the TO phonon can be determined by a direct study of the TO dispersion curve in the long-wavelength approximation [30, 31]. We assume a quadratic dependence of the soft-mode frequency Ω_q with q such as

$$\Omega_q^2 = \omega_0^2 + Dq^2 = \omega_0^2(1 + r_c^2 q^2) \tag{1}$$

where ω_0 is the soft-mode frequency at the zone centre and r_c the correlation length of the mode.

This equation can also be expressed as

$$\Omega_q^2 = \omega_0^2 + (d\xi)^2 \tag{2}$$

with $\xi = (a/2\pi)q$ and $d = (2\pi\omega_0/a)r_c$.

By calculating the parameters ω_0 and d yielding the best adjustment of the dispersion curves, we deduced the length of correlated chains: $n_c = r_c/a$. The results obtained as

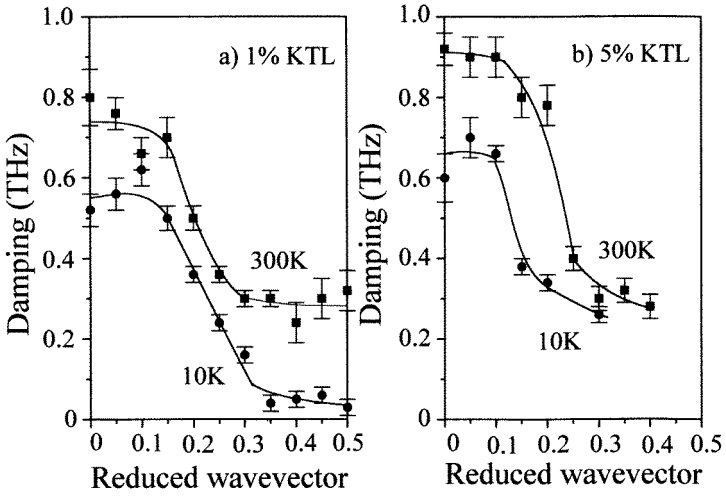

Figure 6. Wavevector dependence of the TO phonon damping at 300 K and 10 K for (a) 1% Li KTL and (b) 5% Li KTL. The lines are guides to the eye.

functions of temperature for 1% Li KTL and 5% Li KTL are reported in figure 7. When the radius r_c is larger than 1, at least three cells are correlated. Our results indicate that, when the wavelength is longer than the correlation length, the phonon damping begins to increase significantly. In particular, for the 1% Li KTL, it should be noted that the strong lowering of the TO_1 phonon linewidth observed in the q-dependence takes place at wavevectors corresponding to wavelengths presenting a magnitude equivalent to the polar cluster dimensions [32, 33]. The shift to lower q-values of this damping lowering observed at 10 K for 5% Li KTL certainly results from the enhancement of the correlation length due to the ferroelectric phase transition. Moreover, the decrease in the TO mode damping at low wavevectors is connected with an increase in the TA mode damping. This phenomenon can be considered to be a consequence of the coupling between the optic and acoustic branches which enhances due to the softening of the TO_1 mode.

4. Theoretical considerations

4.1. The dynamical model

In order to analyse the influence of Li introduction on the non-linear properties of the $KTaO_3$ matrix, we apply the anharmonic lattice dynamic model described by Migoni *et al* [34, 35] and extended by Kugel *et al* [36] on KTN. In this model, the particularly high oxygen ion polarizability is supposed to be anisotropic and non-linear; the oxygen core-shell constant interaction $k_{OB}(T)$ in the O–B chains includes a fourth-order term $k_{OB}^{(4)}$ (where B represents the Ta ion) and is written as the temperature-dependent expression

$$k_{OB}^{(T)} = k_{OB}^{(2)} + \tfrac{1}{2}k_{OB}^{(4)}\langle w_{OB}^2\rangle_T. \tag{3}$$

The thermal average $\langle w_{OB}^2\rangle_T$ of the oxygen displacement in the O–B direction can be written as

$$\langle w_{OB}^2\rangle_T = \frac{\hbar}{2m_0N}\sum_{q,j}\frac{f_\alpha^2(O_{\alpha,j}^q)}{\omega(\boldsymbol{q}, j)}\coth\left(\frac{\hbar\omega(\boldsymbol{q}, j)}{2k_BT}\right) \tag{4}$$

where m_0 is the mass of the oxygen ion, N is the number of $\boldsymbol{q}$ points considered in the summation, k_B is the Boltzmann constant and $\omega(\boldsymbol{q}, j)$ is the frequency of the phonon with branch index j and wavevector $\boldsymbol{q}$. The shell eigenvector components are represented by f_α [35].

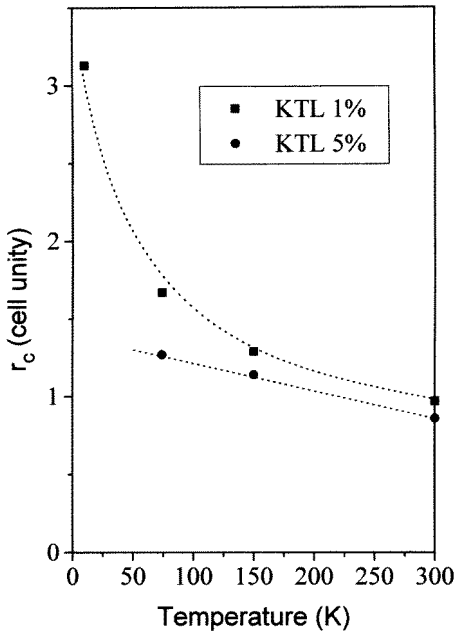

Figure 7. Temperature dependence of the correlation length of the soft mode in 1% and 5% Li KTL in the paraelectric phase.

In our calculations we use the same parameter values as Migoni *et al* [35] and Kugel *et al* [36] have applied to $KTaO_3$ and $KTaO_3$:Nb, respectively. For each temperature and each Li concentration, the lattice dynamical calculations have been done with $k_{OB}(T)$-values fitting the zone centre soft-mode frequency. The suitable $k_{OB}(T)$-value is the value which gives a calculated soft-mode frequency in fair agreement with the experimental soft-mode frequency. These experimental data have been taken from our neutron measurements for 1% and 5% Li KTL and with neutron data available in the literature for pure $KTaO_3$ [16–18].

Since this model is valuable exclusively in the cubic phase, it has been applied only for temperatures higher than 70 K in the case of the 5% Li KTL crystal.

4.2. Phonon dispersion curve calculation

Our dynamical calculations provide a complete set of theoretical dispersion curves in the three high-symmetry directions for different temperatures and concentrations. Figure 8 shows the comparison between the calculated and measured dispersion curves in the [100] direction for different temperatures in 5% Li KTL. Fair agreement is obtained in the whole Brillouin zone for both the TO_1 and the TA modes. The same calculations have been done for 1% Li KTL and have led to the same conclusion.

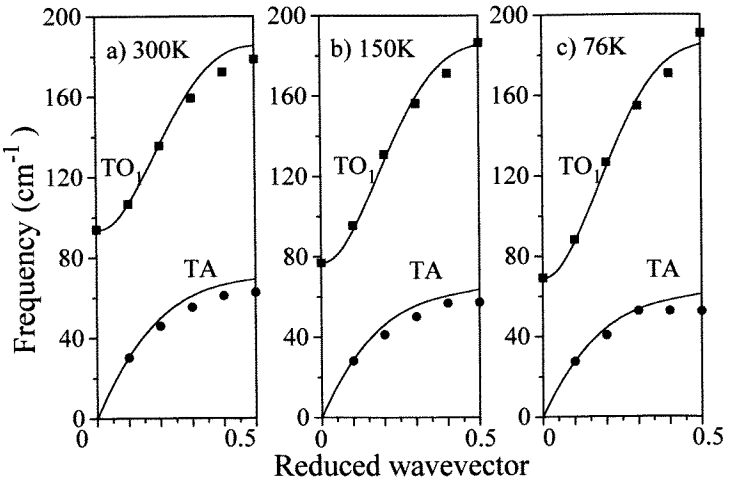

Figure 8. Comparison of the experimental and calculated dispersion curves for 5% Li KTL at (a) 300 K, (b) 150 K and (c) 76 K in the [100] direction: ■, ● , experimental values; ——, calculated values.

4.3. Structure factor calculation

The intensity of the phonon scattering is proportional to $C|F|^2$ where C contains the Debye–Waller factor and phonon frequency and F is the one-phonon structure factor given by the following equation [37]:

$$F = \sum_{\kappa} b_{\kappa} \frac{\boldsymbol{Q} \cdot \boldsymbol{e}_{\kappa}(\boldsymbol{q}, j)}{\sqrt{m_{\kappa}}} \exp(\mathrm{i}\boldsymbol{Q} \cdot \boldsymbol{r}_{\kappa}) \tag{5}$$

where b_κ is the scattering length of the ion κ, r_κ its position in the unit cell and m_κ its mass. $\boldsymbol{\tau}$ is a reciprocal-lattice vector, $\boldsymbol{Q} = \boldsymbol{k}_f - \boldsymbol{k}_i = \boldsymbol{\tau} \pm \boldsymbol{q}$ is the transfer vector and $\boldsymbol{e}_\kappa(\boldsymbol{q}, j)$ is the polarization vector component for the phonon with branch index j and wavevector $\boldsymbol{q}$ of the ion κ.

The comparison of the experimental (after normalization) and calculated phonon scattered intensities obtained in the [100] direction at 300 K for the TO and TA modes is represented in figure 9.

4.4. Calculation of the non-linear oxygen core-shell constant

As detailed in section 4.1, the calculations of the dispersion curves needed a preliminary estimation of the $k_{OB}(T)$-values. Figure 10(a) shows the concentration and temperature dependence of the oxygen core-shell constant interaction $k_{OB}(T)$ used in our calculations. From the phonon frequencies and eigenvectors (equation (4)) we determined the thermal average of the oxygen displacement $\langle w_{OB}^2 \rangle_T$ in the O–B direction. This quantity is reported in figure 10(b) for pure $KTaO_3$ and 1% and 5% Li KTL.

When the Li concentration increases, the $k_{OB}(T)$-value increases and $\langle w_{OB}^2 \rangle_T$ decreases. Both these results are opposite to those observed for KTN [36] and confirm that the non-linear contribution due to the oxygen polarizability in the O–B direction is attenuated by the Li ions. On the basis of the results shown in figure 10 and of equation (3), the variation in the linear $k_{OB}^{(2)}$ and quadratic $k_{OB}^{(4)}$ contributions to the oxygen polarizability with respect

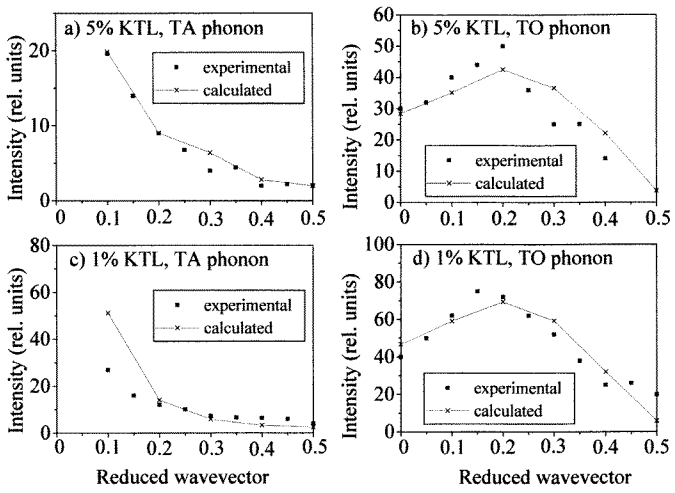

Figure 9. Comparison of normalized experimental and calculated phonon scattered intensities at 300 K for (a) the TA mode in 5% Li KTL, (b) the TO mode in 5% Li KTL, (c) the TA mode in 1% Li KTL and (d) the TO mode in 1% Li KTL.

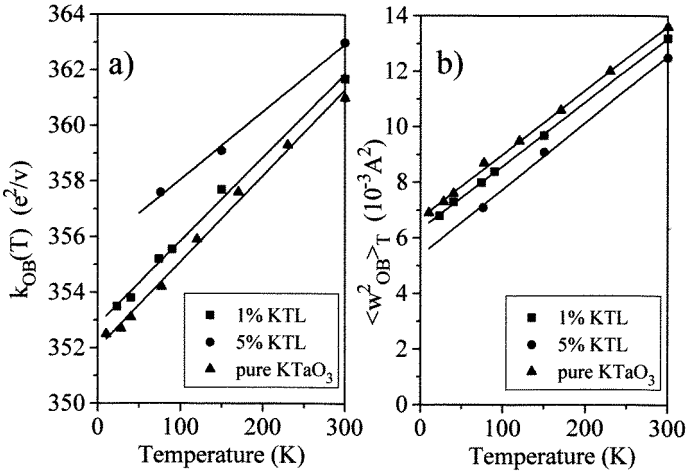

Figure 10. Concentration and temperature dependences of (a) the oxygen core-shell coupling constant $k_{OB}(T)$ and (b) the thermal average of the oxygen shell displacement $\langle w_{OB}^2 \rangle_T$. The lines are guides to the eye.

to the Li concentration can be calculated by least-square fits. The results obtained are reported in figure 11 and show that the harmonic constant $k_{OB}^{(2)}$ remains nearly constant (around 345 e^2/v) in the Li concentration range studied. For comparison, the data obtained for KTN [36] are given in the inset of figure 11. They show that, for KTN with Nb concentration from 0 to 2%, $k_{OB}^{(2)}$ also remains constant around a similar value to that for KTL. Nevertheless, a slow increase in $k_{OB}^{(2)}$ is noted for KTL contrary to the data for KTN where it decreases but very slowly. The non-linear contribution $k_{OB}^{(4)}$ decreases with a rate of 22% for $0\% \leqslant x_{Li} \leqslant 5\%$ contrary to the case of KTN in which the equivalent value

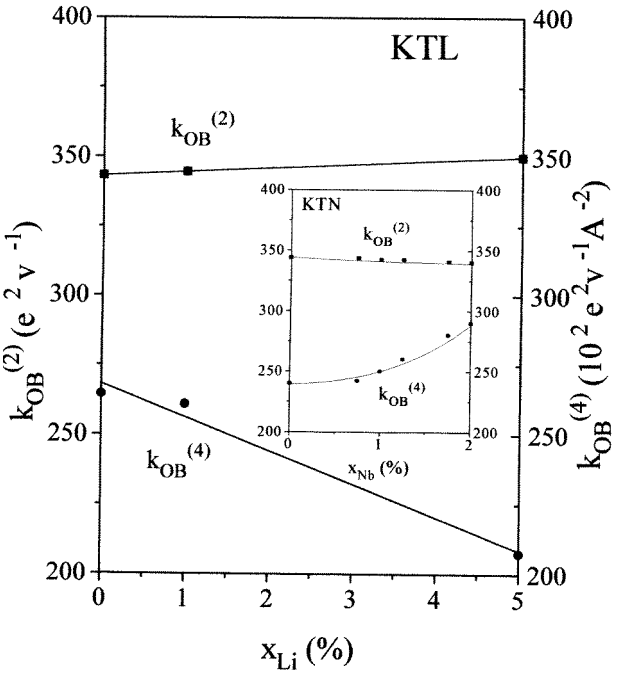

Figure 11. Dependence on Li concentration of the linear and quadratic coupling parameters $k_{OB}^{(2)}$ and $k_{OB}^{(4)}$. The results obtained for KTN [36] are given in the inset for comparison. The lines are guides to the eye.

was increased by the Nb introduction with a rate of about 20% for $0\% \leqslant x_{Nb} \leqslant 2\%$. The complete substitution of Ta by Nb leads, as shown in [36] to a multiplication of $k_{OB}^{(4)}$ by 2.3.

5. Conclusions about the phase transition and the non-linear character of the system

Our neutron measurements presented here are an additional contribution to the understanding of questions which are still open in the KTL system. In the 5% Li doped sample, the results clearly indicate a splitting of the TO_1 and TA branches into two components in all the Brillouin zone at low temperatures. These data are characteristic of a cubic–tetragonal structural phase transition and of long-range order interactions.

In the 1% Li KTL sample, no splitting of the TO branch can be observed at any temperature nor for any wavevector. The low-temperature phase, which is known to exhibit a dipolar glass behaviour, remains cubic.

In accordance with Raman spectroscopy measurements [7], the neutron data show that the mode frequency of the ferroelectric mode is hardened by the Li introduction, contrary to what is observed in the Nb-doped sample.

The particular TO phonon damping behaviour seems to be connected to the correlation length of the soft mode. The comparison with the TA phonon damping is in agreement with the assumption of a coupling between the two modes.

Lattice dynamic calculations fitting these behaviours lead to the fact that the non-linear contribution $k_{OB}^{(4)}$ to the oxygen polarizability decreases when the Li concentration is

enhanced. This means that the Li reduces the non-linearity along the Ta–O chains.

This observation can, in our sense, be explained by the role played by the strong off-centring (about 1 Å) of the Li ions [3] when introduced into the perovskite lattice. The Li off-centring has several consequences: the creation of a dipolar moment directly related to the Li^{+}; the distortion of the lattice structure around the dipoles and, in particular, displacement of the first-neighbour O^{2-} ions [33]; the creation of polar clusters of correlation length depending on the Li content and on the temperature. These effects, described as atomic and electronic distortions, break the straight chain-line in the Ta–O–Ta sequence and impede the huge non-linearities developed along such highly polarizable chains [36]. An effect of the same order on the electronic structure of the O^{2-} ions has been analysed by us [38, 39] in the interpretation of the photoconductivity detected in the KTL system.

Acknowledgment

We would like to express our thanks to A Levelut for providing the KTL samples studied.

References

[1] Höchli U T, Knorr K and Loidl A 1990 *Adv. Phys.* **39** 405
[2] Vugmeister B E, Glinchuk M D 1990 *Rev. Mod. Phys.* **62** 993
[3] Van der Klink J J and Borsa F 1984 *Phys. Rev.* B **30** 52
[4] Andrews S R 1985 *J. Phys. C: Solid State Phys.* **18** 1357
[5] Kleeman W, Kütz S and Rytz D 1987 *Europhys. Lett.* **4** 239
[6] Chase L L, Lee E, Prater R L and Boatner L A 1982 *Phys. Rev.* B **26** 2759
[7] Klein R S, Kugel G E, Fontana M D and Höchli U T 1992 *Ferroelectrics* **125** 325
[8] Prater R L, Chase L L and Boatner L A 1981 *Phys. Rev.* B **23** 5904
[9] Azzini G A, Banfi G P, Giulotto E and Höchli U T 1991 *Phys. Rev.* B **43** 7473
[10] Borsa F, Höchli U T, Van der Klink J J and Rytz D 1980 *Phys. Rev. Lett.* **45** 1884
[11] Christen H M, Höchli U T, Chatelain A and Ziolkiewicz S 1991 *J. Phys.: Condens. Matter* **3** 8387
[12] Höchli U T, Weibel H E and Rehwald W 1982 *J. Phys. C: Solid State Phys.* **15** 6129
[13] Doussineau P, Farssi Y, Fresnois C, Levelut A, McEnaney K, Toulouse J and Ziolkiewicz S 1993 *Europhys. Lett.* **21** 323
[14] Höchli U T, Hessinger J and Knorr K 1991 *J. Phys.: Condens. Matter* **3** 8377
[15] Doussineau P, Frenois C, Levelut A and Zioliewicz S 1994 *J. Physique* **14** 147
[16] Shirane G, Nathans R and Minkiewicz V J 1967 *Phys. Rev.* **157** 396
[17] Comes R and Shirane G 1972 *Phys. Rev.* B **5** 1886
[18] Axe J D, Harada J and Shirane G 1970 *Phys. Rev.* B **1** 1227
[19] Migoni R, Bilz H and Bäuerle D 1978 *Proc. Int. Conf. on Lattice Dynamics* (Paris: Flammarion Sciences) p 650
[20] Yelon W B, Cochran C, Shirane G and Linz A 1971 *Ferroelectrics* **2** 261
[21] Chou H, Shapiro S M, Lyons K B, Kjems J and Rytz D 1990 *Phys. Rev.* B **41** 7231
[22] Fontana M D, Kugel G E and Foussadier L 1993 *Europhys. Lett.* **23** 427
[23] Fontana M D, Kress W, Kugel G E, Lehner N and Rytz D 1984 *Ferroelectrics* **55** 23
[24] Kamitakahara W A, Loong C K, Ostrowski G E and Boatner L A 1987 *Phys. Rev.* B **35** 223
[25] Maglione M, Höchli U T, Joffrin J and Knorr K 1989 *J. Phys.: Condens. Matter* **1** 1527
[26] Toulouse J and Hennion B 1994 *Phys. Rev.* B **49** 1503
[27] Vogt H and Uwe H *Phys. Rev.* B **29** 1030
[28] Kugel G E, Vogt H, Kress W and Rytz D 1984 *Phys. Rev.* B **30** 985
[29] Fontana M D, Dolling G, Kugel G E and Carabatos C 1979 *Phys. Rev.* B **20** 3850
[30] Lines M E and Glass A M 1977 *Principles and Applications of Ferroelectrics* (Oxford: Clarendon)
[31] Uwe H, Lyons K B, Carter H L and Fleury P A 1985 *Phys. Rev.* B **33** 6436
[32] Di Antonio P, Vugmeister B E, Toulouse J and Boatner L A 1993 *Phys. Rev.* B **47** 5629
[33] Stachiotti M G, Migoni R L and Höchli U T 1991 *J. Phys.: Condens. Matter* **2** 4341
[34] Migoni R L, Biltz H and Bauerle D 1976 *Phys. Rev. Lett.* **37** 1158
[35] Migoni R L, Currat R, Perry C H and Axe J D 1985 private communication

[36] Kugel G E, Fontana M D and Kress W 1987 *Phys. Rev.* B **35** 813
[37] Bruesch P 1982 *Phonon: Theory and Experiments II (Springer Ser. Solid State Sci. 34)* (Berlin: Springer) p 159
[38] Klein R S, Kugel G E, Glinchuck M D, Kuzian R O and Kondakova I V 1994 *Phys. Rev.* B **50** 9721
[39] Klein R S, Kugel G E, Glinchuck M D, Kuzian R O and Kondakova I V 1995 *Opt. Mater.* **4** 163